Ultrasound assisted liquid-liquid extraction in microchannels-A direct contact method

John, Jinu Joseph; Kuhn, Simon; BRAEKEN, Leen & Van Gerven, Tom (2016)
Ultrasound assisted liquid-liquid extraction in microchannels-A direct contact method.
In: CHEMICAL ENGINEERING AND PROCESSING, 102, p. 37-46.

DOI: 10.1016/j.cep.2016.01.003
Handle: http://hdl.handle.net/1942/26519

Ultrasound assisted liquid–liquid extraction in microchannels—A direct contact method

Article *in* Chemical Engineering and Processing · January 2016

DOI: 10.1016/j.cep.2016.01.003

4 authors, including:

Jinu Joseph John
University of Leuven
5 PUBLICATIONS **20** CITATIONS
SEE PROFILE

Simon Kuhn
University of Leuven
58 PUBLICATIONS **769** CITATIONS
SEE PROFILE

Tom Van Gerven
University of Leuven
218 PUBLICATIONS **4,295** CITATIONS
SEE PROFILE

Ultrasound assisted liquid-liquid extraction in microchannels - A direct contact method

Jinu Joseph John[1], Simon Kuhn[1], Leen Braeken[2], Tom Van Gerven[1,*]

[1]Process Engineering for Sustainable Systems (ProcESS), Department of Chemical Engineering, KU Leuven, Belgium

[2]KU Leuven Lab4U - Faculty of Industrial Engineering, Agoralaan Building B bus 8, B-3590 Diepenbeek, Belgium

Abstract

A new method to apply ultrasound to a microchannel for liquid-liquid extraction was explored. The microchannel tubes are subjected to the ultrasound by direct contact with the transducer without the presence of a liquid medium. The design was constructed with the objectives of reproducibility, proper control of the ultrasound parameters and visibility of the behaviour of the two phase flow under the influence of ultrasound throughout the length of the channel. Two mechanisms of emulsion formation were observed. The effectiveness of the system under the influence of various operating and design parameters was quantified by calculating the yields of the two phase hydrolysis reaction of *p*-nitrophenyl acetate. The behaviour under various frequencies and amplitude was explored. At a frequency of 20.3 kHz, amplitude of 840mV and flow rate of 0.1ml/min the highest increase in yield was observed, which was almost 2.5 times that of the silent condition. A comparison was also made against silent batch and flow conditions to determine the actual effectiveness of the system. To obtain an identical yield of 75% the required residence time could be reduced by a factor of 20 in the sonicated flow condition compared to the silent batch condition.

1. Introduction

Liquid-liquid extraction is a common and important unit operation in any chemical industry. There have been many innovative technologies developed to carry out this process in the most efficient manner. A recent development is the use of microreactors. There is an increasing interest in microreactors because of their advantages [1–4] of large interfacial area per unit volume, shorter diffusion lengths, increased mixing effects by the formation of internal circulations and enhanced heat transfer. When two immiscible liquids are admitted into a microchannel, different flow patterns are generated depending on the fluid properties and operating conditions [5]. In certain situations the advantage of the increased interfacial area and mixing effects may not be sufficient enough to balance the short residence time. Many methods have been developed to increase the mixing effects in a microreactor which are broadly classified as active and passive ones [6]. Ultrasound is an example of the active approach, providing a non-contact method of mixing [7] within the very small structures of the microreactor. The advantages of using ultrasound in chemical synthesis and in microstructured devices for multiphase flow have been reported in literature [8–13].

Ultrasounds are sounds waves with frequencies larger than 20 kHz. When these sound waves are applied to a liquid medium cavities are formed which in turn cause many chemical and physical effects such as

---

[*] Corresponding author: Tom Van Gerven, tel.: +32 16 322342, e-mail: tom.vangerven@cit.kuleuven.be

acoustic streaming, jet formation and local hot spot generation [13]. In this research, the physical effects are pursued, mainly the improved mixing by the vibration of the bubbles created by cavitation and the shockwaves created by implosion of the cavitation bubbles [14]. When two immiscible phases are subjected to ultrasound an emulsion of the two phases is created [10,11,15]. Hubner et al. report the formation of vibrating bubble clusters in the dispersed phase which disturb the interface by creating jets of the dispersed phase to move into the continuous phase, thus causing an emulsion formation [10]. This experiment was done in a glass capillary placed on a sonotrode, wherein the continuous phase was the aqueous phase and the organic phase was dispersed. In this paper it is further explored whether this mechanism persists in the reverse flow condition of the [10,11] aqueous phase being the dispersed phase and the organic phase being the continuous one by using a hydrophobic plastic tubing.

There are various designs available for coupling microstructured devices with ultrasound. The common approach is the utilization of the ultrasound bath [8,9] to achieve good transfer of the ultrasound vibrations. In ultrasound baths the area of maximum intensity is determined by various techniques like hydrophones and calorimetric tests. Knowing this area the microstructure is then suspended in these defined locations and the ultrasound is applied. There are several disadvantages associated with the ultrasound bath concept. Firstly, there is always loss of ultrasound intensity in the liquid transfer medium (i.e. the water bath), for which Hübner et al. [10] made use of pressure to minimize the cavitational activity in the transfer medium. Secondly, as each ultrasound bath behaves differently with respect to the regions of high ultrasound intensity, this also creates difficulties for reproducibility and comparability between different reactors reported in literature. Thirdly, since all these reactors have the microstructure suspended in the liquid medium, it is difficult to observe what exactly happens to the two phase immiscible systems when ultrasound is applied. Finally, the suspension of the microstructure in the region of maximum intensity can itself cause a change of the field which results in the regions in which the reactors are suspended to be no more the areas of high intensities.

The scope of this work is therefore to develop a method for applying ultrasound to a microchannel under conditions of reproducibility, good control of the ultrasound parameters and visibility of the process during the entire operation to better study the influence of ultrasound on two phase flow. We therefore moved away from the ultrasound bath concept and focused on the development of a direct contact device where the ultrasound transducer is directly in contact with the microstructured device without passing via a liquid volume.

2. Materials and Methods

2.1 Reactor Design

A novel design was developed (Figure 1), which utilizes the direct coupling of the ultrasound transducer to the microstructured device without the help of a liquid medium. The transducer is bolted on to an aluminium plate of size 80X80 mm and 4 mm thickness. The size of the plate was selected based on the diameter of the transducer which is 78 mm. Aluminium was chosen because the front element of the transducer is made out of aluminium and less attenuation of the ultrasound signal is occurring when using materials with the same acoustic impedance. Square channels are cut in the plate with channel dimensions matching the reactor tubing to be placed inside the channels. The distance between the 4 parallel channels is selected based on the bending radius of the tubing (i.e. 14 mm)

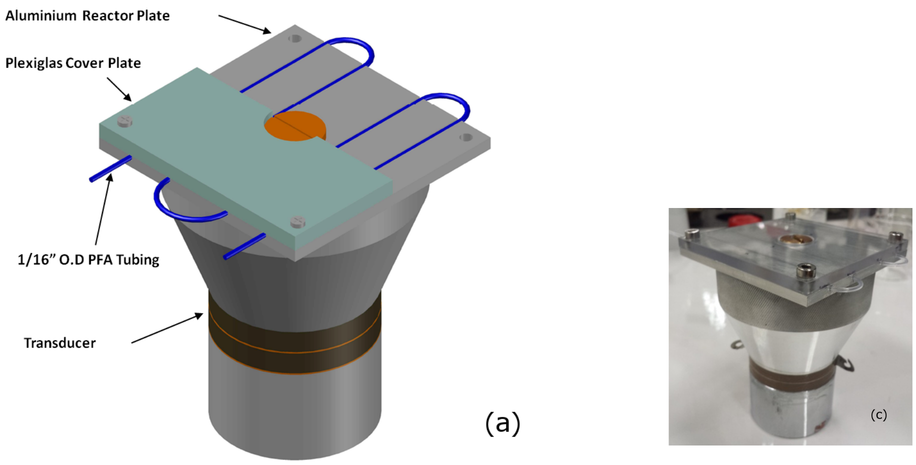

Figure 1: (a) Schematic representation of the reactor, (b) Side section of single channel, (c) Complete reactor.

PFA (Perfluoroalkoxy copolymer) was selected as tubing material as it is chemically inert and transparent allowing a clear view on the behaviour of the two phase system flowing inside. The tubing has an outer diameter of 1.58 mm diameter and inner diameter of 0.80 mm. The tubing is held in place in the channels by a Plexiglas cover plate that is screwed on the aluminium plate at the four corners. Plexiglas is selected due to its transparency and because it is a sound soft material, thereby avoiding damage during the application of ultrasound. Since the idea here is to transfer the ultrasound vibrations by direct contact, the reactor is named as Direct Contact Type Ultrasound Reactor.

2.2 Experimental Setup

The experimental setup consists of two syringe pumps that pump the aqueous and organic phases through a T-junction with a selected flow rate (between 0.1 and 1.0 ml/min) to form the desired flow pattern. In all flow rates that are selected the slug flow persists. In all the experiments both the aqueous and the organic streams are pumped at the same flow rate (i.e. phase ratio 1:1). The total length of tubing used is 58 cm out of which the first 9 cm constitute the distance from the T-junction to the reactor plate, the next 40 cm the sonicated section and 9 cm the distance from the reactor plate outlet to the separating flask. From the T-junction the two phase system flows into the designed reactor after which 2 ml of the phases is collected in a separating flask and separated by gravity separation.

The ultrasound wave characteristics frequency, amplitude and shape of the wave are controlled by a Picotest G5100A waveform generator. The signal is sent to the transducer through an E&I 1020L RF amplifier. The transducer is a multi frequency type which can operate at frequencies of 20, 40 & 60 kHz (Ultrasonics World MPI-7850D-20-40-60 H). A cooling fan is used to keep the transducer cool, to avoid variations in power and to avoid overheating of the reactor plate. The entire setup is shown in Figure 2.

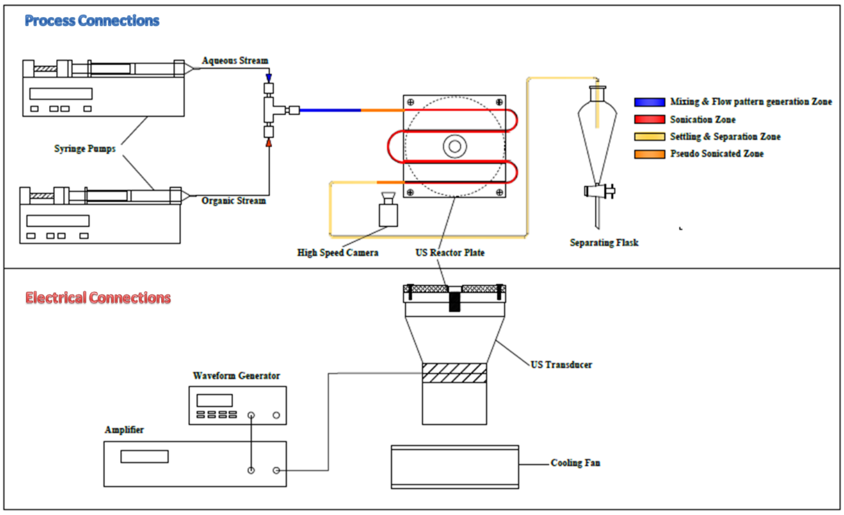

Figure 2: Experimental setup.

In all experiments that were conducted except for the variation in amplitude the absorbed power or the net applied power of the transducer reactor assembly was kept constant. This is the difference between the forward and reflected power as indicated by the amplifier. The forward power is the actual applied power, but a part of the power is reflected back as a result of the change in impedance of the reactor assembly whereas the waveform generator, amplifier and the connection all have a constant impedance of 50 ohms. Due to the nature of the reactor design, It is not trivial to determine the mechanical energy or the acoustic energy that is really delivered to the two phase system.

2.3 Reaction

The reaction that is utilized for defining the performance of the reactor is the hydrolysis of *p*-nitrophenyl acetate [10,16,17].

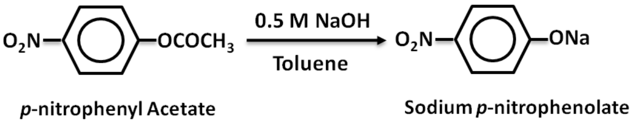

Figure 3: Hydrolysis reaction of *p*-nitrophenyl acetate.

This is a reactive extraction process (Figure 3). The *p*-nitrophenyl acetate is hydrolysed by a NaOH solution to produce sodium *p*-nitrophenolate, which is soluble in the aqueous phase. In terms of the process streams the organic phase consists of the *p*-nitrophenyl acetate dissolved in toluene at a concentration of 0.05 M, while the aqueous phase consists of a 0.5 M NaOH solution. This is an instantaneous reaction and hence it is mass transfer controlled. As an excess of NaOH is used, this reaction can be considered as a pseudo-first order reaction. When the sodium *p*-nitrophenolate is dissolved in water, the solution turns yellow, which can be utilized to quantify its concentration in a UV-1601 Shimadzu spectrophotometer at a wavelength of 400 nm.

3. Results & Discussion

3.1 Effect of ultrasound on two phase flow

On a macroscopic level upon sonication an emulsion is formed between the phases as expected [10,11]. The emulsion formation limits itself to the dispersed phase. The regularity of the two phase slug flow is completely disturbed, as the slugs are no longer moving along with the continuous phase at a regular interval and size. As soon as the slug flow reaches the sonicated section emulsification starts. The emulsified bubbles also tend to coalesce with the neighbouring emulsified bubbles to form very irregularly sized slugs (Figure 4).

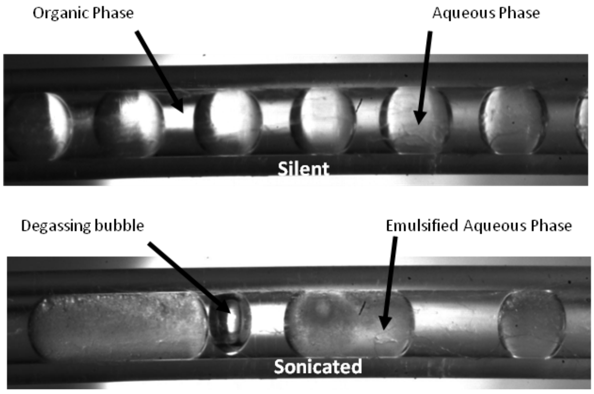

Figure 4: Silent and sonicated two phase system (Images recorded at the exit of the reactor plate).

Based on the different activity in the various regions of the tubing, we can define different sections (Figure 2): 1) the mixing zone (in this zone there is only formation of segmented flow and mixing as a result of this segmented flow; this is purely a non sonicated zone), which consists of the T-Junction and the initial 1-4 cm (depends on the length of the pseudo-sonicated zone) of the tubing before the reactor 2) the sonicated zone which consists of the tubing placed in the aluminium reactor plate and 3) the settling region which consists of the tubing after the reactor plate till the separating flask. In addition to these regions there is also 4) a pseudo-sonicated zone which is the part of the tubing before the entry and after the exit of the reactor. The total length from the T-junction to the reactor plate is 9 cm, the length of the pseudo-sonicated zone is between 5 and 8 cm depending on the power that is applied in the reactor, which leaves a length of the mixing zone between 1 and 4 cm.

On a microscopic level the behaviour of ultrasound on the two phase flow was studied by using a high speed camera (Photron Fastcam Mini UX-100). It was observed that when the slug flow nears the reactor plate, i.e in the pseudo sonicated zone, minute bubbles form in the continuous phase (Figure 5 (ii)) which tend to either assemble into clusters or coalesce to form large bubbles that are of the size of the diameter of the tubing. In the case of cluster formation, the bubble clusters tend to vibrate at the interface of the aqueous and the organic phase (Figure 5 (b)). Since this occurs while the bubble is still moving the clusters vibrate and move along the entire length of the dispersed phase, starting first at the hemispherical part and moving along the cylindrical interface (Figure 5 (c)). This disturbance of the interface causes jets of the continuous phase to move into the dispersed phase resulting in very fine emulsions (Figure 5 (d)). This mechanism show a similarity with the initial formation of a bubble cluster in the organic phase as reported by Hübner *et al.* [10], but the preceding steps of the cluster crossing the interface and dispersing out in the aqueous phase are different, which could be associated with the inverse flow regimes in the two studies (aqueous phase being the continuous phase in Hübner *et al*[10]., but the dispersed phase in this study).

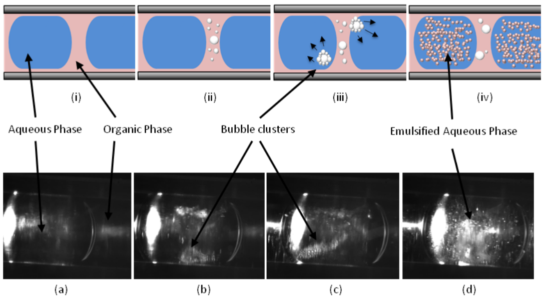

Figure 5:Bubble cluster initiation (a to d - 0.21 s)

The alternative observed phenomenon is the large bubble initiation. Since the solvents are not degassed, large ellipsoidal bubbles are formed whose diameters almost equal the internal diameter of the tube (Figure 6(a)). The large bubble tends to vibrate along the interface and pushes against it (Figure 6(b)), after which it passes over the entire cylindrical interface of the dispersed phase (Figure 6 (c),(d)), resulting in jets of the continuous phase moving into the dispersed phase causing an emulsion. In most of the cases it is observed that the large bubble initiation is also followed by the cluster initiation.

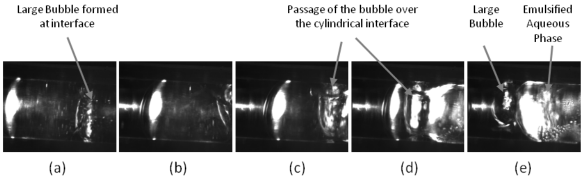

Figure 6 : Large bubble initiation (a to e - 0.178 s).

When ultrasound is applied to a liquid medium there are usually two types of cavitation: transient or stable[18]. In transient cavitation the micro bubbles formed persist only for a short duration and collapse violently. They are usually filled with the vapour of the liquid in which they are formed. In stable cavitation the bubbles formed persist for a longer time and are usually due to the presence of gas inside them. The above described phenomena show a clear non-adherence to the transient cavitation, as both the clusters and the large bubbles persist for a longer period of time. These bubbles can be stable cavitation bubbles or just degassing bubbles as sometimes the large bubbles persist for the entire length of the tubing. Hence the emulsion activity is a result of either vibrating stable cavitation or degassing.

3.2 Effect of operating and design parameters

Experiments were performed to study the influence of each of the operating (amplitude, frequency) and design conditions (flow rate). The performance of the reactor for the various applied conditions is quantified by the yield of the hydrolysis reaction.

3.2.1 Variation of amplitude

To study the effect of the wave amplitude, the experiments were performed at a constant frequency of 20.3 kHz and constant aqueous and organic flow rates of both 0.5 ml/min. The results are displayed in Figure 7. The power mentioned here is the net applied electrical power. When the amplitude is increased, the applied power increases as well. The yield is less affected by the increase in power up to an amplitude of 600 mV, after which there is a steep increase till 840 mV.

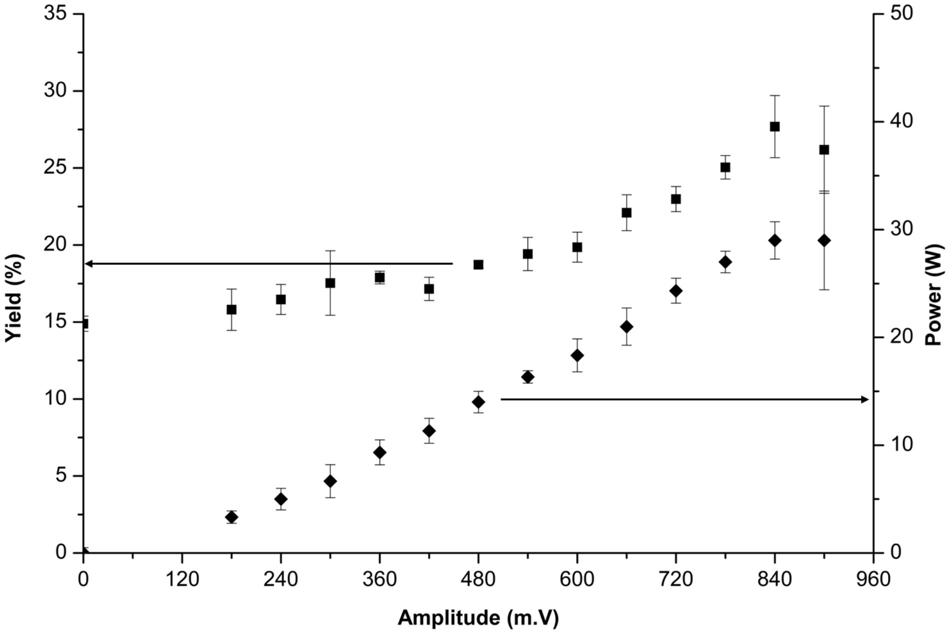

Figure 7: Effect of the variation of amplitude on net electrical power and yield (constant flow rate of 0.5 ml/min). Error bars calculated on the basis of three replicates. (If no error bars are visible they are smaller than the symbol)

Above 600 m.V the increase in yield with power can be attributed to the emulsion formation, which results in a higher interfacial area per unit volume and hence a higher yield. The augmented emulsion formation with increasing power was indeed visually observed by the increased bubble activity and formation of thicker emulsion. The little or no variation of yield below 600 m.V can be the result of the system needing a minimum amount of applied power for there to be an effective influence on the heterogeneous system as there is very little emulsion formation. Beyond 840 mV there is a large variation in the power and yield. This can be attributed to the transducer reaching its power limit at this amplitude, as the operating power limit for the transducer is 100 W and the forward power at 900 mV was measured to be around 99 ± 2 W. The amplitude of 840 mV, equalling an applied electrical power of 29 W, will therefore be utilized for the following experiments as it gives the highest yield for the above selected set of conditions.

3.2.2 Variation of flow rate

The effect of flow rate is studied at a constant frequency of 20.3 kHz , amplitude of 840 mV and applied electrical power of 29 W (where the forward power is at 84±2W). In each of the flow rate variations the flow rate of both the aqueous and organic are kept equal, thus at a 1:1 ratio. The result of the variation of flow rate for the silent and sonicated conditions is shown in Figure 8(a). The flow rates shown are the individual flow rates of each phase and not the total flow rate. The range of Reynolds number in the explored flow rate is between 5.9 and 56.5. In all the explored flow rates it can be seen that the sonicated condition results in higher yield compared to the silent condition.

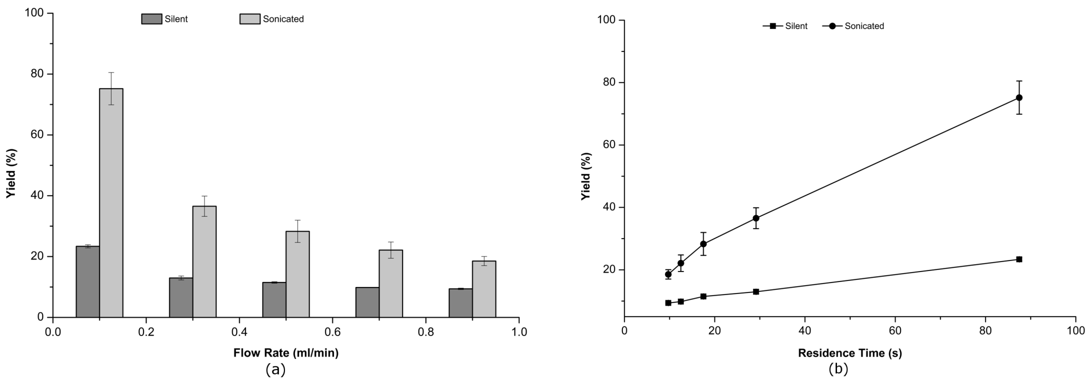

Figure 8: The effect of sonication on yield for constant frequency (20.3 kHz) and amplitude (840m.V) (a) variation of flow rate (b) The variation with corresponding mean residence times for the flow rates Error bars are calculated based on three replicates. (If no error bars are shown they are smaller than the symbol).

We also see a decreasing trend in the yield with increasing flow rate. This is to be expected as increasing flow rate decreases the residence time in the reactor (Figure 8 (b)). In all these flow rates we are still in the laminar regime.

3.2.2.1 Estimation of the volumetric mass transfer coefficient

The volumetric mass transfer coefficients $K_l a$ were calculated for this reaction utilizing the method proposed by Ramshaw and Burns [19], wherein the transfer rates of the p-nitrophenyl acetate between the aqueous and organic slugs can be given by

$$\frac{dC}{dt} = K_l a . \Delta C \qquad [1]$$

where ΔC is the concentration difference between the organic and aqueous phase. As an excess of NaOH is used and since this reaction is instantaneous it can be assumed that all the p-nitrophenyl acetate entering the aqueous phase is consumed completely.

Therefore, $\Delta C = C_{org} - C_{aq} \approx C_{org}$

The equation then becomes

$$\frac{dC}{dt} = K_l a . C_{org} \qquad [2]$$

Solving the above we obtain the volumetric mass transfer coefficient as:

$$K_l a = -\frac{1}{t} \ln (1 - \alpha) \qquad [3]$$

Where α is the portion of p-nitrophenyl consumed.

Equation 3 is solved for $K_l a$ for the various flow rates assuming the transfer time t to be equal to the residence time τ as the system has not reached its equilibrium state. The equilibrium state referred to here is the maximum yield that can be obtained for the reaction, which can be as high as 87% as observed by Hübner *et al.*[10] for the same system. The variation of $K_l a$ with flow rate is plotted in Figure 9 for the average yield values obtained.

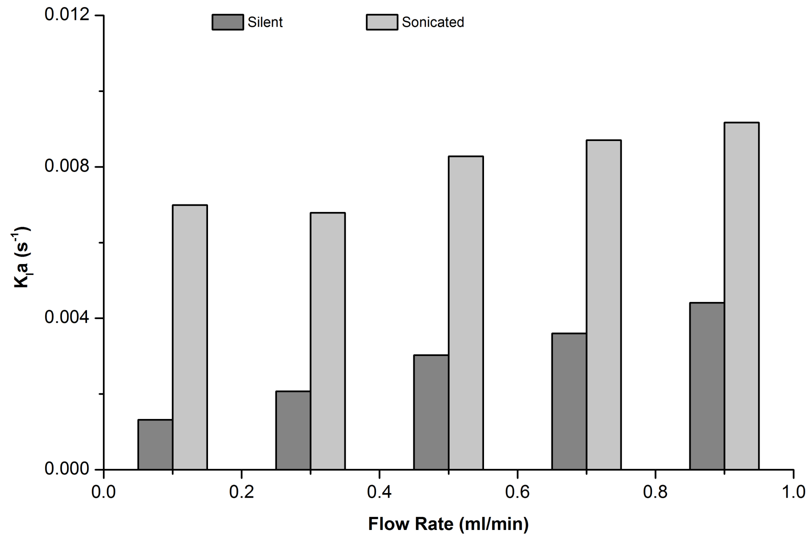

Figure 9: Effect of flow rate and sonication on volumetric mass transfer coefficient for constant frequency (20.3 kHz) and amplitude (840mV).

There is a clear increase in the volumetric mass transfer coefficient by sonication. The lowest flow rate shows the highest improvement in the volumetric mass transfer coefficient upon sonication. In silent condition it is observed that the volumetric mass transfer coefficient increases with increase in the flow rate which can be explained on the basis of the increase in the internal circulation of the liquid slug observed by Kashid et al. [3] as a result of the increase in shear between the wall surface and the liquid with increase in flow rate. A similar behaviour is observed for the sonicated systems but at flow rates higher than 0.3 ml/min. For the lowest flow rate of 0.1 ml/min the $K_l a$ values are slightly higher than at 0.3 ml/min as this flow rate has the highest residence time of 87 s in the flow rates or in other words is sonicated for the longest time among all the flow rates, which promotes better mixing and larger interfacial areas as a result of more opaque emulsion formation. The effect of the sonication on the volumetric mass transfer coefficent seems to be more pronounced for the lowest flow rate of 0.1ml/min and the fact that this effect is not carried to the next flow rates can be a result of the difference in residence times between the flow rates. Between 0.1 ml/min and 0.3 ml/min the residence times decreases by a factor of 3 but between the higher flow rate the decrease in residence times is less than 1.6. Also the largest increase in the $K_l a$ value of 5.3 times is observed for 0.1 ml/min.

3.2.3 Variation of frequency

When comparing frequency, one would like to keep the incoming power constant. It was not trivial to determine the calorimetric power in the reaction liquid due to the difficulty in determining the contribution to heat input by conduction from the transducer to the liquid. A fair comparison between the various frequencies is therefore achieved by keeping the input conditions of the wave (amplitude and net applied electric power) constant. Suitable frequency points were obtained (20.3 kHz, 42.3 kHz & 61.61 kHz) for the same amplitude of 600 mV and net applied power of 20 W (where the forward power is at 49±1 w). The results are shown in Figure 10.

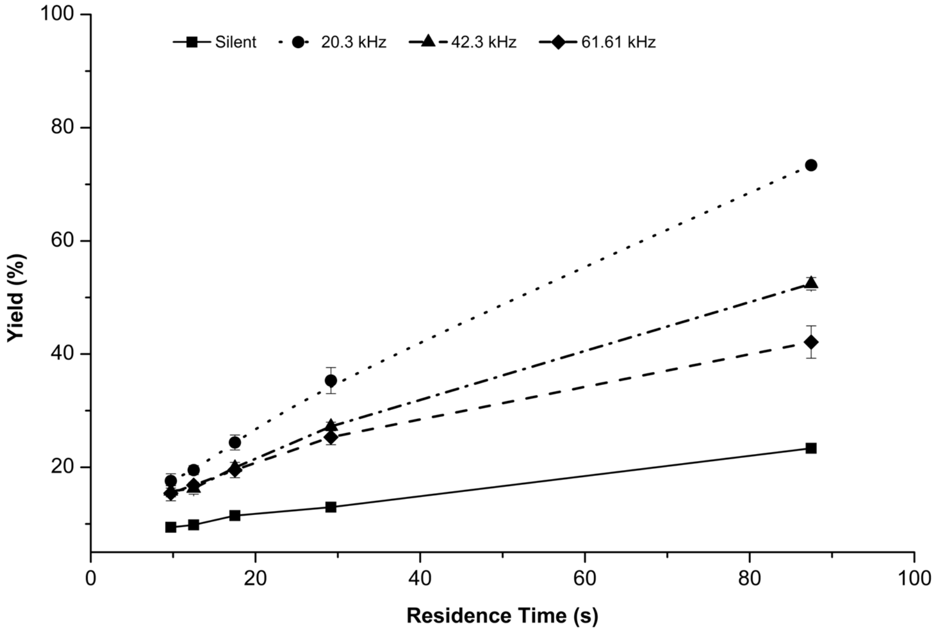

Figure 10: Effect of applied frequency on yield for constant applied power of 20 W. Error bars are based on triplicate measurements. (If no error bars are shown they are smaller than the symbol)

From the results it is evident that for all the explored frequencies the sonicated system gave a higher yield compared to the silent condition. The highest yield was obtained with the lowest frequency. To better understand this effect experiments were conducted using water and the temperature difference between the inlet and outlet streams of the reactor plates were measured at the experimental conditions for a constant flow rate of 0.5 ml/min. This gave rise to the following results, were the highest temperature difference was at 20.3 kHz (10.9 °C), followed by the frequency of 42.3 kHz (9.2 °C) and 61.61 kHz (5.4 °C). First experiments were conducted at the highest temperature rise of 10.9 °C in silent condition at the same flowrate to see if this was a temperature effect, but this resulted in an improvement of 10 % in the yield but in sonicated condition the yield was improved by almost 52 %. Hence the variation in the yield doesn't seem to be purely a temperature effect. But, looking at the temperature difference as an indication of the power transferred to the system it makes sense that the highest yield would be for the 20.3 kHz, followed by the 42.3 kHz and 61.61 kHz.

3.3 Comparison with conventional process

To evaluate the extent of the improvement by ultrasound the sonicated experiments were compared to silent batch conditions as well as silent conditions in a microchannel of the same material and diameter. The non-sonicated batch experiments were performed by taking equal quantities of the aqueous and the organic phases (5 ml) in a conical flask, mixing them by a magnetic stirrer for different residence times and letting it settle before taking samples in the aqueous phase. The results are shown in Figure 11.

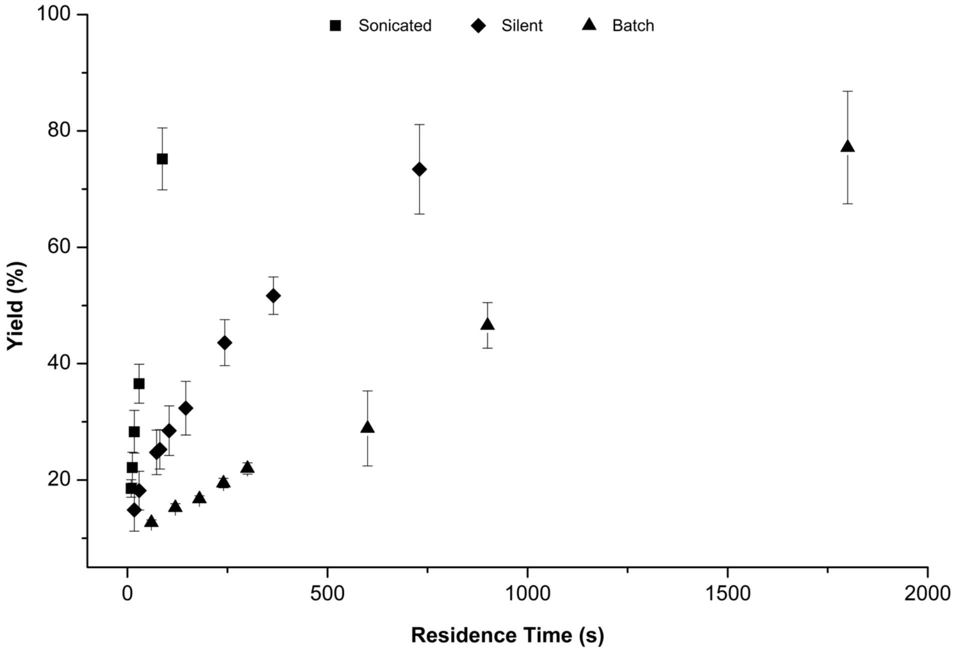

Figure 11: Comparison of silent batch, silent flow and sonicated flow (20.3 kHz, 840 mV) on the yield as a function of residence time. Error bars based on the measurement of three replicates. (If no error bars are visible they are smaller than the symbol)

From the results it can be seen that there is a considerable decrease in required residence time to obtain the same yield by moving from silent batch to sonicated flow conditions. To obtain a yield of 75 %, the required residence time in the sonicated flow reactor was reduced by a factor of 20 in comparison to the batch conditions and by a factor of 8.5 compared to the silent microchannel conditions.

Although this system has been explored by Hübner *et al.* [10] and Ahmedomer *et al.* [8] in the sonicated condition, a clear comparison cannot be made as the method of application of ultrasound and the parameters of the ultrasound waves used vary considerably.

4. Conclusion

A direct method for the application of ultrasound to a microchannel for a two phase flow was explored and a suitable reactor was designed with the appropriate controls for the ultrasound parameters. The emulsion formation mechanism was explored which showed an indirect influence of the ultrasound. The bubbles formed by the application of ultrasound vibrate along the interface to bring about the disruption of the interface resulting in emulsion formation. The bubbles formed are seen to be result of stable cavitation or degassing. The experiments conducted at a frequency of 20.3 kHz, amplitude of 840 mV, input electrical power of 29 W and flow rate of 0.1 ml/min gave the highest yield of 75 %. This also increases the volumetric mass transfer coefficient of the system by a factor of 5.3. When compared to silent conditions in a conventional microchannel, the required residence time to obtain a yield of 75 % was reduced by a factor of 8.5. This method provides a very clearly improvement to the liquid-liquid extraction process in a microchannel.

5. Acknowledgements

The research leading to these results has received funding from the European Community's Seventh Framework Programme (FP7/2007-2013) under grant agreement n◦NMP2-SL-2012-309874 (ALTEREGO).

6. Notation

Latin

a	Interfacial area per unit volume	m^2/m^3
C	Reactants' concentration	mol/m^3
C_{aq}	Reactants' concentration in the aqueous phase	mol/m^3
C_{org}	Reactants' concentration in the organic phase	mol/m^3
K_l	Mass transfer coefficient	m/s

Greek

α	Fraction of the reactant consumed	-
τ	Residence time	s

7. Bibliography

(1) Kashid, M. N.; Renken, A.; Kiwi-Minsker, L. *Chem. Eng. Sci.* **2011**, *66* (17), 3876–3897.

(2) Kashid, M. N.; Agar, D. W. *Chem. Eng. J.* **2007**, *131* (1–3), 1–13.

(3) Kashid, M. N.; Gerlach, I.; Goetz, S.; Franzke, J.; Acker, J. F.; Platte, F.; Agar, D. W.; Turek, S. *Ind. Eng. Chem. Res.* **2005**, *44* (14), 5003–5010.

(4) Ghaini, a.; Kashid, M. N.; Agar, D. W. *Chem. Eng. Process. Process Intensif.* **2010**, *49* (4), 358–366.

(5) Kashid, M.; Kiwi-Minsker, L. *Chem. Eng. Process. Process Intensif.* **2011**, *50* (10), 972–978.

(6) Hessel, V.; Löwe, H.; Schönfeld, F. *Chem. Eng. Sci.* **2005**, *60*, 2479–2501.

(7) Katou, H.; Miyake, R.; Terayama, T. *JSME Int. J. Ser. B* **2005**, *48* (2), 350–355.

(8) Ahmedomer, B.; Barrow, D.; Wirth, T. *Chem. Eng. J.* **2008**, *135*, S280–S283.

(9) Aljbour, S.; Tagawa, T.; Yamada, H. *J. Ind. Eng. Chem.* **2009**, *15* (6), 829–834.

(10) Hübner, S.; Kressirer, S.; Kralisch, D.; Bludszuweit-Philipp, C.; Lukow, K.; Jänich, I.; Schilling, a; Hieronymus, H.; Liebner, C.; Jähnisch, K. *ChemSusChem* **2012**, *5* (2), 279–288.

(11) Aljbour, S.; Yamada, H.; Tagawa, T. *Chem. Eng. Process. Process Intensif.* **2009**, *48* (6), 1167–1172.

(12) Riccaboni, M.; La Porta, E.; Martorana, A.; Attanasio, R. *Tetrahedron* **2010**, *66* (23), 4032–4039.

(13) Fernandez Rivas, D.; Cintas, P.; Gardeniers, H. J. G. E. *Chem. Commun. (Camb).* **2012**, *48* (89), 10935–10947.

(14) Mason, T. J. *Chem. Soc. Rev.* **1997**, *26*, 443–451.

(15) Jackson, W.; Bondy, B. Y. C.; Sollner, K. *Trans. Faraday Soc.* **1935**, *31*, 835–843.

(16) Ahmed, B.; Barrow, D.; Wirth, T. *Adv. Synth. Catal.* **2006**, *348* (9), 1043–1048.

(17) Ahmed, B.; Barrow, D. A.; Wirth, T. **2008**, 2–4.

(18) Cravotto, G.; Cintas, P. *Chem. Soc. Rev.* **2006**, *35* (2), 180–196.

(19) Burns, J. R.; Ramshaw, C. *Lab Chip* **2001**, *1* (1), 10–15.